Simulating Seasonal Evolution of Subglacial Hydrology at a Surging Glacier in the Karakoram

Journal:	*Journal of Glaciology*
Manuscript ID	JOG-2025-0011.R3
Manuscript Type:	Article
Date Submitted by the Author:	13-Jun-2025
Complete List of Authors:	Narayanan, Neosha; Georgia Institute of Technology, ; Massachusetts Institute of Technology, Sommers, Aleah; Dartmouth College, Thayer School of Engineering Chu, Winnie; Georgia Institute of Technology Steiner, Jakob; University of Graz Faculty of Natural Sciences, Siddique, Muhammad; Information Technology University Meyer, Colin; Dartmouth College, Thayer School of Engineering Minchew, Brent; Massachusetts Institute of Technology, Department of Earth, Atmospheric and Planetary Sciences
Keywords:	Glacier modelling, Glacier hazards, Glacier hydrology, Glacier surges, Mountain glaciers
Abstract:	Glacier motion, retreat, and glacier hazards such as surges and glacial lake outburst floods (GLOFs) are likely underpinned by subglacial hydrology. Recent advances in subglacial hydrological modeling allow us to shed light on subglacial processes that lead to changes in ice mass balance in High Mountain Asia (HMA). We present the first application of the Subglacial Hydrology And Kinetic, Transient Interactions (SHAKTI) model on an alpine glacier. Shishper Glacier, our study site, is a mountain glacier in northern Pakistan that exhibits concurrent surges and GLOFs which endanger local communities and infrastructure. Without coupling to ice velocity, the modeled subglacial hydrological system undergoes transitions between inefficient to efficient drainage and back during spring and fall, supporting previous observations of spring and fall

	speedups of glaciers in the region. We compare modeled effective pressures from the years 2017-2019 with previously observed velocities, suggesting that while subglacial hydrology may explain seasonal sliding dynamics, our model is unable to provide an explanation for surge-scale behavior, implicating a need for coupled hydrological and ice dynamics modeling of surge conditions. This work demonstrates the potential of using ice sheet models for alpine glaciology and provides a new nucleus for modeling of glacial hazards in alpine environments.

Journal of Glaciology, Vol. 00, No. 0, 0000 1

Simulating Seasonal Evolution of Subglacial Hydrology at a Surging Glacier in the Karakoram

Neosha NARAYANAN,[1,2] Aleah N SOMMERS,[3] Winnie CHU,[1] Jakob STEINER,[4,5] Muhammad Adnan SIDDIQUE,[6] Colin R MEYER,[3] Brent MINCHEW[2]

[1] *Department of Earth and Atmospheric Sciences, Georgia Institute of Technology, Atlanta, GA, USA*

[2] *Department of Earth, Atmospheric, and Planetary Sciences, Massachusetts Institute of Technology, Cambridge, MA, USA*

[3] *Thayer School of Engineering, Dartmouth College, Hanover, NH, USA*

[4] *Himalayan University Consortium, Lalitpur, Nepal*

[5] *Institute of Geography and Regional Science, University of Graz, Austria*

[6] *Information Technology University, Lahore, Pakistan*

Correspondence: Neosha Narayanan <nnarayanan38@gatech.edu>

ABSTRACT.

Glacier motion, retreat, and glacier hazards such as surges and glacial lake outburst floods (GLOFs) are likely underpinned by subglacial hydrology. Recent advances in subglacial hydrological modeling allow us to shed light on subglacial processes that lead to changes in ice mass balance in High Mountain Asia (HMA). We present the first application of the Subglacial Hydrology And Kinetic, Transient Interactions (SHAKTI) model on an alpine glacier. Shishper Glacier, our study site, is a mountain glacier in northern Pakistan that exhibits concurrent surges and GLOFs which endanger local communities and infrastructure. Without coupling to ice velocity, the modeled subglacial hydrological system undergoes transitions between inefficient to efficient drainage and back during spring and fall, supporting previous observations of spring and fall speedups of glaciers in the region. We compare modeled effective pressures from the years 2017-2019 with previously observed velocities, suggesting that while subglacial hydrology may explain seasonal sliding dynamics,

our model is unable to provide an explanation for surge-scale behavior, implicating a need for coupled hydrological and ice dynamics modeling of surge conditions. This work demonstrates the potential of using ice sheet models for alpine glaciology and provides a new nucleus for modeling of glacial hazards in alpine environments.

INTRODUCTION

The High Mountain Asia (HMA) region, known as the "Third Pole," contains the largest concentration of ice outside of the polar ice sheets. The glaciers of HMA feed major water systems which provide water and sanitation for over a billion people (Scott and others, 2019). In particular, the Karakoram is the most heavily glaciated mountain range in Asia (RGI Consortium, 2017) and is a critical water source for large parts of Pakistan and parts of northern India (Scott and others, 2019). However, climate change has led to increasingly negative mass balance, putting the area's future at risk (Zhang and others, 2023a; Shean and others, 2020; Rounce and others, 2020; Bolch and others, 2011). Glacial lake outburst floods (GLOFs) in the region have also caused significant loss of human lives and infrastructure damage in recent decades (Shrestha and others, 2023), and the risk of exposure to local communities and infrastructure due to growing proglacial lakes may potentially increase (Zhang and others, 2023b, 2024; Zheng and others, 2021; Harrison and others, 2018). GLOFs in the Karakoram region occur through breaches of moraine or ice dams, which are associated with rapid (re)-organization of subglacial waters and channels (Nye, 1976; Gudmundsson and others, 1995; Bigelow and others, 2020; Kingslake and Ng, 2013; Flowers and others, 2004). Proglacial and proximal (ice-dammed) lakes, which are often hydraulically connected with the subglacial drainage network, also exert an important boundary condition on the subglacial water network (Bigelow and others, 2020; Anderson and others, 2005; Armstrong and Anderson, 2020)).

The Karakoram region is also home to a high concentration of surge-type glaciers (Sevestre and Benn, 2015; Copland and others, 2009, 2011). Surges are a phenomenon characterized by cyclical, order-of-magnitude accelerations of glaciers that can be sustained for months to years (Eisen and others, 2001; Jay-Allemand and others, 2011; Round and others, 2017; Bhambri and others, 2020; Björnsson, 1998). They occur in geographical clusters that fall in "climatic envelopes" that may provide favorable temperatures and accumulation rates for surge motion (Sevestre and Benn, 2015; Jiskoot and others, 2000). Surges are also associated with till deformation (Minchew and Meyer, 2020; Minchew and others, 2016). Buildups of basal water pressure are thought to play a role in the initiation and sustenance of surge motion (e.g., Kamb (1987); Flowers and others (2011); Björnsson (1998); Jay-Allemand and others (2011)). However, the causes of surge behavior remain unclear as not all surging glaciers seem to be directly attributable to changes in mass-balance state or thermal regime (e.g., Liu and others (2024); Murray and others (2000)).

Subglacial hydrology controls ice velocity through changes in effective pressure, defined as the difference between the overburden pressure and the and water pressure at the bed (Nienow and others, 2005). Seasonal variations in subglacial hydrology modulate ice sheet and glacier velocities (Hart and others, 2022; Sommers and others, 2024; Schoof, 2010; Zwally and others, 2002; Iken and others, 1983). Numerous studies have shown that the velocity of glaciers increases during melt seasons (e.g., Nanni and others (2023); Zwally and others (2002); Hart and others (2022); Bhambri and others (2020)). In alpine glaciers of HMA, observed regional speedups have been proposed to occur due to changes in subglacial drainage efficiency. In particular, these glaciers can also exhibit a pattern of speedups in both the spring and fall (Beaud and others, 2022; Nanni and others, 2023). These studies suggest that these seasonal speedups occur due to increases in meltwater production and subsequent lubrication at the ice-bed interface.

While surges and outburst flooding have for the most part been investigated as separate phenomena, multiple studies in the Karakoram have observed GLOFs to occur concurrently with transitions in surge motion, suggesting that subglacial hydrology may play a non-straightforward role in the synchronous timing of these events (Beaud and others, 2021; Bhambri and others, 2020; Bazai and others, 2022a; Round and others, 2017; Bazai and others, 2022b; Steiner and others, 2018). Understanding the role that subglacial hydrology plays in the severity and timing of these hazards could improve early warning systems for water availability and outburst flooding. While several in-situ observational studies have been conducted and are in progress (e.g., Gilbert and others (2020); Miles and others (2021, 2019); Pritchard and others (2020)) there are very few direct observations of subglacial hydrology in HMA. Therefore, in this study, we lay the groundwork for investigating the role of subglacial hydrology in ice dynamics and outburst flooding through modeling.

We focus on Shishper Glacier (36.40°N 74.61°E) in the eastern Karakoram range in Pakistan (Fig. 1). The glacier has also been referred to in literature as Shisper and Shishpare. Located in the Hunza Valley in Gilgit-Baltistan, Pakistan, Shishper is part of a surge and lake drainage system with another glacier to its west, called Muchuwar (also previously spelled as Muchuhar or Mochowar). The two glaciers were

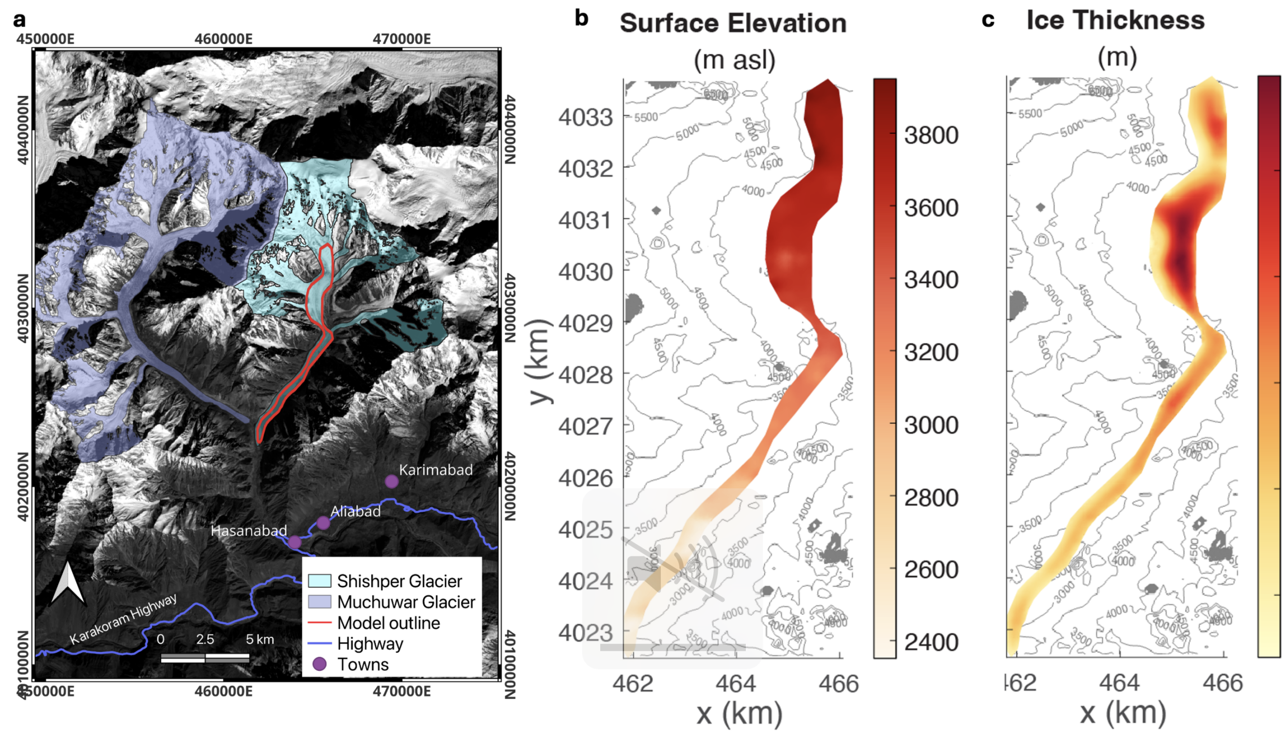

Fig. 1. (a) Outlines of adjacent valley glaciers Shishper and Muchuwar (Randolph Glacier Inventory Version 6.0) overlaid on Landsat 8 OLI NIR imagery from December 2016. Our modeled domain is outlined in red. (b) Surface elevation from TanDEM-X 90m DEM, with contours showing the terrain elevation in meters. (c) Ice thickness from Millan and others (2022)'s global dataset. All coordinates are projected to WGS 84/UTM Zone 42N.

connected prior to 1950, when the two separated (Muhammad and others, 2021). Shishper's main trunk is approximately 7 km long and is fed by several tributary glaciers at the northeast (upper-elevation) side. In total, the glacier is about 15 km in length.

Both Shishper and Muchuwar have surged cyclically for as long as observations have been recorded, since the early 1900s (Beaud and others, 2021). Shishper underwent major surges in 1973, 2000-2011 and most recently between 2017-2019 (Bhambri and others, 2020). During this time, the terminus advanced approximately 1.5 km (Bhambri and others, 2020). In June 2019, the surge and subsequent lake drainage resulted in the closing of two power plants, the evacuation and considerable damage of some houses in the downstream village, lasting damage to agricultural land, and finally the destruction of the main road bridge crossing the stream, affecting transport along the main transport axis in the region. In mid-November 2018, the advancement of Shishper blocked meltwater flow from Muchuwar Glacier, which created an ice-dammed proximal lake (Beaud and others, 2022). This lake tends to fill up in November-December and in May to a depth of 30-80m, with an estimated volume of 30 million m^3. When the lake drains, the outburst flood drains through Shishper's terminus and down into the valley below. The maximum river flow observed at the downstream village of Hassanabad is 150-200 m^3 s^{-1}, compared to a base flow of about 20 m^3 s^{-1} (Muhammad and others, 2021). After the lake is filled in the winter, drainage occurs more gradually, as opposed to the spring filling which results in a more dramatic drainage of the lake.

In this study, we simulate the seasonal dynamics of the subglacial drainage system of Shishper Glacier in isolation from velocity coupling and lake drainage. We use a state-of-the-art subglacial hydrology model, forced with realistic meltwater inputs, to gain insight into the evolution of the water flow and pressure distribution beneath the glacier. The following sections describe the modeling methods and assumptions, meltwater forcing data, simulation results, and limitations of the approach.

MODEL SETUP AND ASSUMPTIONS

To simulate the subglacial hydrological system of Shishper Glacier, we employ the SHAKTI (Subglacial Hydrology and Kinetic, Transient Interactions) model (Sommers and others, 2018), which is implemented in the Ice-sheet and Sea-level System Model (ISSM) (Larour and others, 2012). The current implementation of SHAKTI in ISSM is the simplified formulation from Sommers and others (2023) which neglects englacial storage, opening by sliding, and melt due to changes in the pressure melting point. SHAKTI is capable of modeling a variety of network systems between the end-member cases of efficient and inefficient drainage systems. It does this by allowing the hydraulic transmissivity to vary spatially and temporally (Sommers and others, 2018, 2023). In addition, it accounts for varying laminar, turbulent, and intermediate flow regimes (Sommers and others, 2018).

The model domain is traced from the Randolph Glacier Inventory, Version 6.0 (RGI Consortium, 2017). The tributary branches of Shishper Glacier, located above about 3500 m asl, likely experience less liquid precipitation and decreased melting compared to the lower section of the main trunk and therefore may not contribute significantly to the subglacial hydrological system. Our aim is to examine the evolution in the hydrology in the main trunk, rather than evaluating the exact quantity of subglacial water in the system; for these reasons, we reserve including hydrological contributions from the tributary glaciers for future work. Furthermore, we neglect frictional heating due to basal sliding, which may decrease the flux of meltwater through the hydrological system; however, our intention is to isolate the effects of seasonal melt on the drainage system, so we also reserve calculation of melt from frictional sliding for future work. The modeled hydrological domain overlaid on the RGI 6.0 outline is shown in Fig. 1, depicting a glacier outline from 2016, before the 2017-2019 surge event. We focus on modeling the subglacial hydrology for a steady geometry, with the glacier outline and ice thickness held constant throughout the simulations.

To obtain surface and bed geometries for the glacier, we use the TanDEM-X global DEM (German Aerospace Center, 2018) along with a global glacier thickness dataset (Millan and others, 2022). Glacier thickness is subtracted from surface elevation to obtain a bed topography, and all spatial data are projected to WGS 84/UTM Zone 42N. Radar mapping of subglacial topographies and glacier thicknesses at other glaciers have revealed large uncertainties associated with this ice thickness dataset, which was calculated using mass conservation techniques (Tober and others, 2024; Millan and others, 2022). In addition, it is likely that artificially smooth bed topographies calculated from mass conservation inversions may affect the results of subglacial hydrology simulations MacKie and others (2021). Due to the lack of in-situ observations to validate Millan and others (2022)'s dataset, we emphasize that the exact routing of subglacial channels in our simulations is subject to the uncertainty associated with the estimated bed topography.

We manually trace the model domain to the RGI outline using in-built functionality in ISSM. The DEM and bed topography data are interpolated onto a 2-dimensional unstructured triangular mesh with 40 m resolution. The ideal mesh size and geometry were determined after conducting a winter equilibration for 600 days at varying mesh sizes (shown in Appendix). We conclude from these tests that the location of channel formations is insensitive to mesh size. The 40 m resolution, which yields a mesh containing 3302 vertices and 6035 elements, provides enough detail and numerical stability while saving on computational costs. The mesh provides the basis for the P1 triangular Lagrange finite element solver used by SHAKTI. We test 20 slightly varying domain outlines with slightly different variations in domain outline, conducting a winter equilibration wherein all subglacial water is generated by basal melt (see section "Establishing Winter Base State") for 1000 days on each. The final geometry used for the transient simulations is chosen based on the criteria that mean ice-bed gap height, gap-integrated basal water flux (the approximate momentum equation for water velocity integrated over the gap height - see Sommers and others (2018)), and effective pressure equilibrate after 1000 days without anomalous numerical artefacts near corners or curvatures. The ice velocity is set to 0 throughout all of the transient simulations, isolating the seasonal evolution of subglacial hydrology without frictional heating feedbacks from basal sliding. All simulations in this work are carried out with ISSM Version 4.23 using a MATLAB interface on MacOS.

Surface Melt Timeseries

To estimate timing and magnitude of seasonal meltwater inputs to the bed, we use the European Centre for Medium-Range Weather Forecasts (ECMWF)'s Reanalysis v5 (ERA5) (Muñoz-Sabater and others, 2021) as inputs to Litt and others (2019)'s temperature-indexed ice melt model to obtain spatio-temporally varying estimates for surface melt across the domain (Fig. 2). These ERA5 weather data are based on an array of field stations and weather models (Setchell, 2020), and directly provide estimates for snow cover, air temperature, and total liquid precipitation across the five years (Muñoz-Sabater and others, 2021). Ice melt across the mesh is calculated using the temperature index (TI) melt parametrization from Litt and others (2019) (Fig. 2). We calculate daily melt over ice when the glacier surface is bare (using a temperature index of 6.5 mm ºC^{-1} day^{-1}, computed from values from Litt and others (2019) and melt from snow for pixels that are snow covered (using an index of 4.1 mm ºC^{-1} day^{-1}, following Braithwaite (2008)). We scale the relative fraction of ice and snow melt per pixel using the relative snow cover data. While melt or surface runoff from rainfall from outside the model domain may also reach the model domain and eventually the glacier bed, we do not consider these inputs here. The TI model is shown to be more accurate for glaciers below 3500 m above sea level (a.s.l) (Litt and others, 2019), which is where most of Shishper's tongue is located (Fig. 1). ERA5 data was downscaled from its native 9 km to the model resolution (50 m) using a Kriging interpolation (Kusch and Davy, 2022). While some in-situ climate data is available in the region, no station was operational in the vicinity of the glacier; using in-situ data from an off-glacier station far away from the glacier would introduce its own set of uncertainties. Due to the relatively high temporal (1 day) and spatial (1 deg^2) resolutions, ERA5 data provide the best available estimate of meltwater inputs to the bed. SHAKTI is able to represent meltwater inputs as either point inputs or as distributed inputs; in this study, we apply the ERA5 melt estimate as spatially distributed input over the bed, which is appropriate for heavily crevassed glaciers such as Shishper. The strong hydraulic coupling between surface and basal meltwater environments (Miles and others, 2017; Zwally and others, 2002; Iken and Bindschadler, 1986; Shepherd and others, 2009; Gulley and Benn, 2007) has given us justification to make the assumption that all meltwater inputs to the bed (i.e., surface melt, rainwater, aquifer contributions) are instantaneous. Furthermore, the broken-up and crevassed nature of Shishper's surface could allow for quicker delivery of meltwater to the bed.

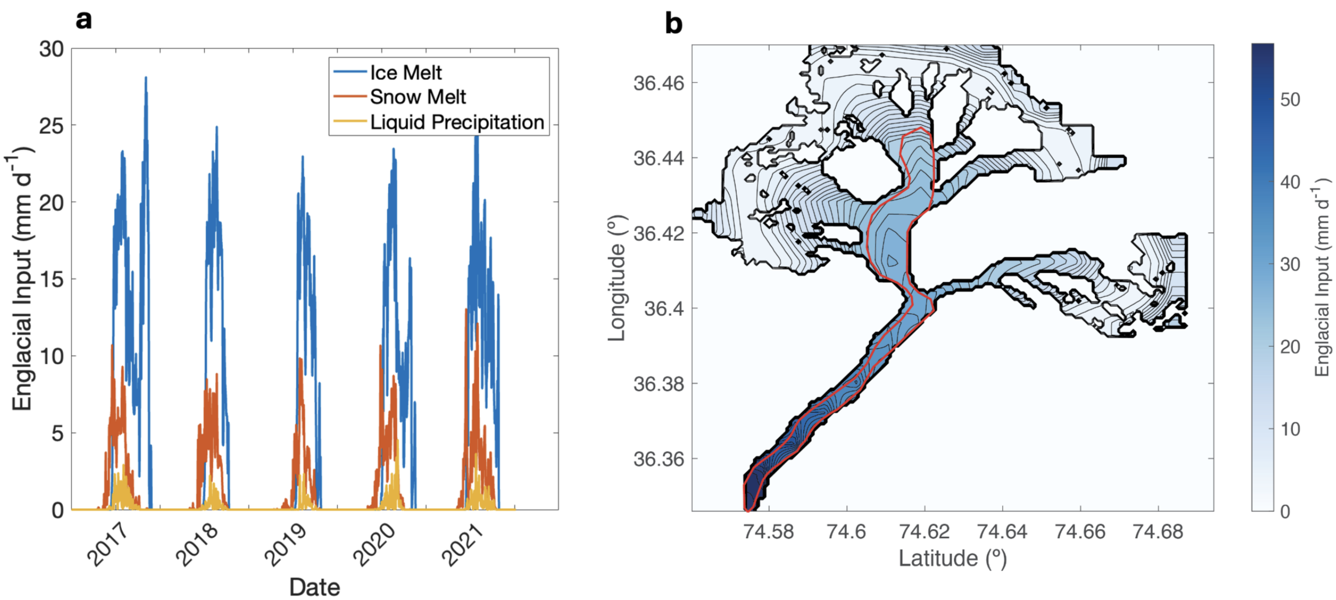

Fig. 2. (a) Englacial inputs to the transient subglacial hydrology model, averaged over the glacier, as calculated by ERA-5 Land and the temperature-indexed ablation model. (b) Average englacial input during the 2017 melt season (May through September). The red outline indicates the modeled domain.

TRANSIENT GLACIER HYDROLOGY SIMULATIONS

Establishing Winter Base State

Before transient simulations can be run, the base winter state of the hydrological system must be established. To do this, we allow the drainage system to develop with zero external meltwater to the bed. During the winter, we assume that there is no surface or englacial melt, with geothermal flux and turbulent dissipation as the only sources of meltwater at the bed. Geothermal heat flux is set to 70 mW m^{-2}, which is within previously measured values in the area (Shengbiao and Jiyang, 2000). Note that we have prescribed sliding velocity to be zero, so there is no frictional heating or cavity opening from sliding over bumps. Because we exclude all contributions from tributary glaciers, a Neumann boundary condition of zero flux is applied to all lateral edges of the domain. A Dirichlet boundary condition is applied to the near-terminus domain boundary, with hydraulic head equal to the bed elevation (i.e. water pressure equal to atmospheric pressure at the outflow). A time step of 1 day is used for obtaining the final equilibrated state.

We define equilibrium by assessing the time rate of change of gap height, basal water flux, hydraulic head, and effective pressure. We deem the model "equilibrated" if there is no visible growth or decay in the minimum, maximum, and spatial mean values of each of these parameters after 500 days; for example,

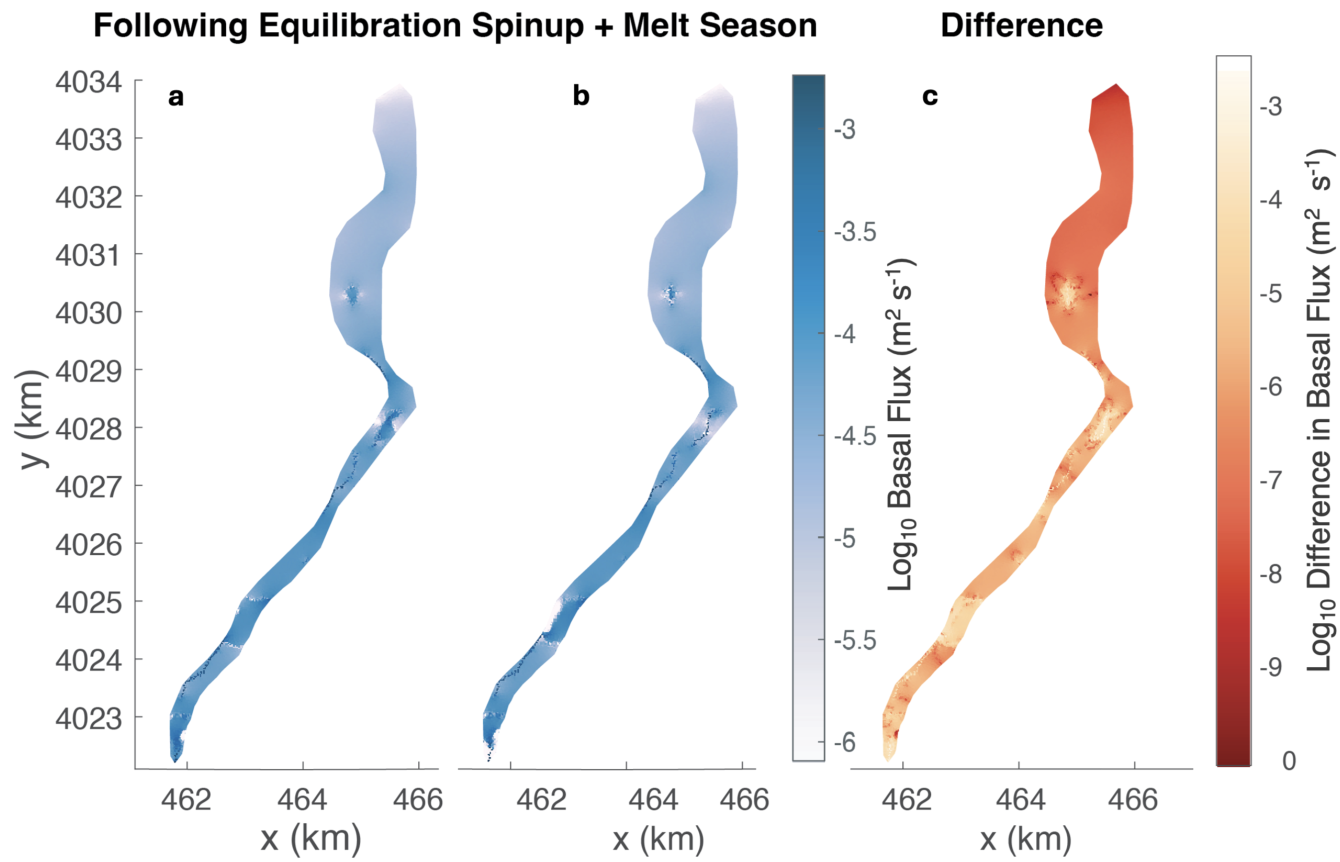

Fig. 3. Basal flux across the modeled domain following (a) a "winter state" equilibration spinup with no melt inputs to the system (b) a transient simulation through a full calendar year including a summer melt season and return back to frozen winter conditions. (c) The difference between the two equilibrated states.

mean effective pressure changes at a constant rate of approximately 2e-7% per year at the end of the winter equilibration. Once all output parameters reach equilibrium, after approximately 600 days, there is formation of a primary drainage channel down the main trunk of the glacier (Fig. 3a). It is also worthwhile to note that the channel has formed in the absence of any surface water melt, indicating its potential to persist through the winter months just given a small amount of meltwater from geothermal flux and turbulent dissipation.

Beginning from the base winter state (Fig. 3a), we run a transient simulation of 1 year (January 1 - December 31). Following this year, the model reaches a new stable winter state (Fig. 3b). The second stable state is largely similar to the first, but shows more efficient, concentrated drainage at a few areas including the terminus and up-glacier at 4028 km N. Running additional melt seasons yields no additional changes in winter drainage patterns, indicating a new equilibrium. This perennial channel then forms the basis for the subglacial system during the melt season.

Seasonal Evolution of Subglacial Hydrology

To understand how Shishper's subglacial drainage network responds to seasonal changes in meltwater flux, we run transient simulations across a period of five years, 2017-2021, using a timestep of 30 minutes. The transient input for these simulations is the temporally and spatially varying sum of ice melt, snow melt, and liquid precipitation (Fig. 2), applied as distributed meltwater inputs to the subglacial system throughout our model domain of the main glacier trunk. Potential incoming melt inputs from tributary glaciers are not included.

Fig. 4 illustrates changes in the configuration of the drainage system throughout 2017, which is representative of the pattern observed across all five years. We see a mostly closed system in winter (Fig. 4b) which transitions to a highly efficient, channelized system at the peak of the melt season (Fig. 4c). The basal flux mirrors the surface melt input trend, peaking around August (Fig. 2a), while hydraulic head and effective pressure stay mostly steady apart from spikes at the beginning and end of the melt season. At the height of the melt season, the drainage system extends to the northernmost part of the domain, splitting into arborescent patterns characteristic of channelized drainage (Röthlisberger, 1972). By October 5, these channels then disappear, with the upper part of the system having completely shut down. Finally, the system returns to the winter state by late October (Fig. 4d and e).

The lower channel which traverses the mid- to lower trunk clearly persists through every simulated winter in 2017-2021, and can be seen in both images of the "closed" state (Fig. 4a, d, and e). We know that this channel appears during the winter equilibration, during which time the only water at the ice-bed interface comes from turbulent dissipation and geothermal heat flux. There is always a consistent stream of water, although small, that keeps the main channel open. Bhambri and others (2020) show that surface melt elevations move from 6400 m in peak summer to 3500 m at the end of winter (no surface melt is observed in December, January, or February) meaning that the bottom part of the glacier will always receive more melt, and is more likely to contain channels, than the top.

Fig. 5 presents a closer look at the rapid decreases in effective pressure at the beginning of the melt season (May-July). As shown in Fig. 5a, coming from primarily distributed winter drainage with low transmissivity, the rise in hydraulic head due to the system's inability to transport growing fluxes, and the rapid fall in head back to the equilibrium value, show that the system resolves spikes in water pressure by developing more efficient pathways (i.e. increasing transmissivity by opening new channels). The calculated spikes in hydraulic head in Figs. 4 and 5 are higher than realistic physical values, in which localized buildups

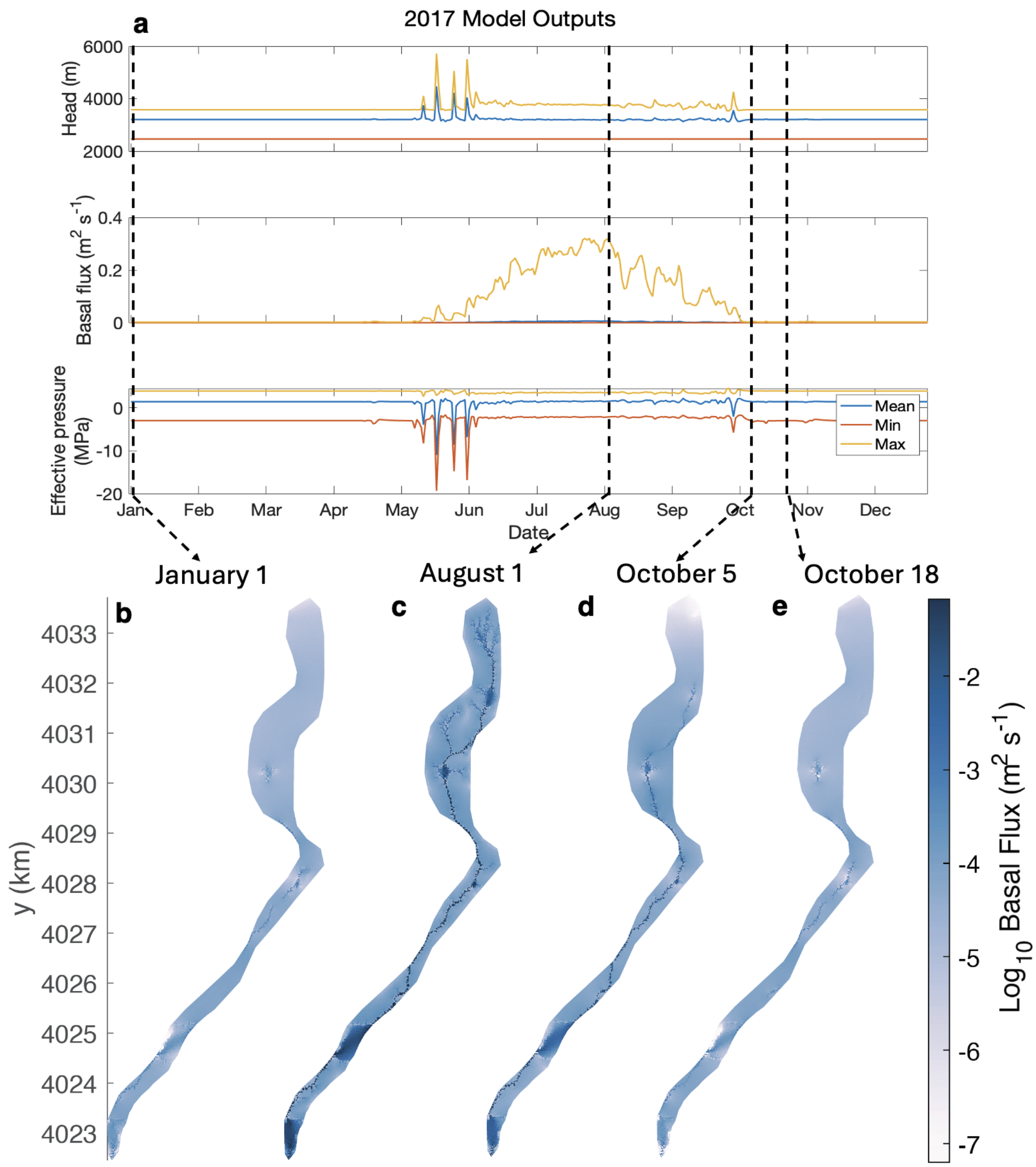

Fig. 4. (a) Model outputs for 2017 including hydraulic head, basal flux, and effective pressure. Mean, min, and max refer to the spatially averaged mean and the minimum and maximum values over the mesh. (b) Log_{10} basal flux across the glacier at four times during the year: January 1 (winter), August 1 (peak melt), October 5 (drawdown of drainage network at the end of the melt season), and October 18 (return to winter conditions).

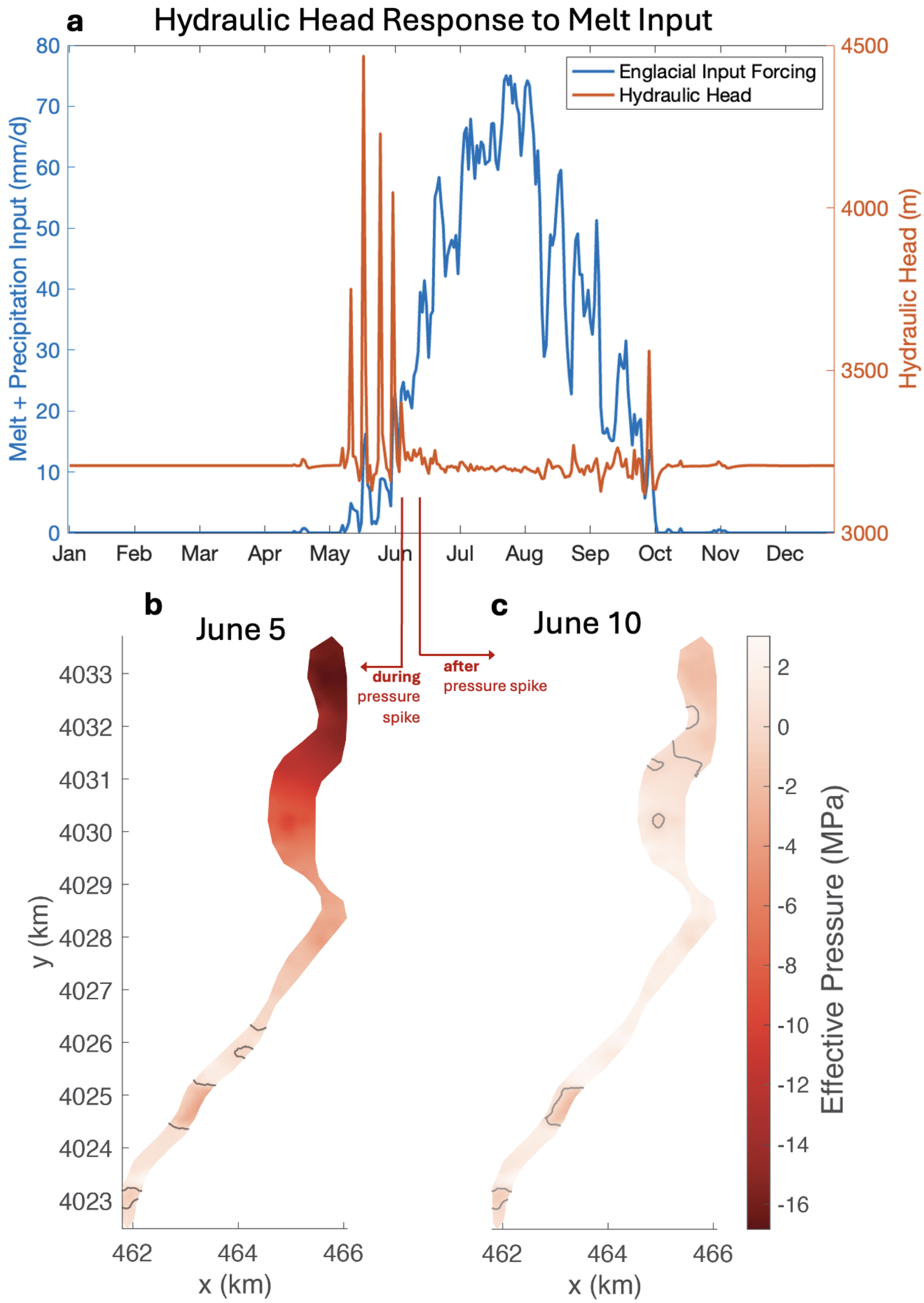

Fig. 5. Top: (a) Melt input (blue) overlaid with spatially averaged hydraulic head (red) during 2017. Bottom: pressures across the mesh during (b) and after (c) the spike in hydraulic head in early June. Gray contours indicate effective pressure of 0 MPa (flotation, where ice overburden equals water pressure).

of very high water pressure would more quickly be resolved through hydraulic jacking (local uplift where water pressure exceeds flotation) and/or fracturing of the overlying ice. Since these processes are not explicitly represented within SHAKTI, localized large water pressures may be resolved more slowly in the simulations, thus appearing as non-physical values. Setting a warmer ice temperature may also result in less extreme spikes (see Appendix C). Such a buildup of hydraulic head can be observed in Fig. 5b (June 5), where a large area of negative N (high water pressure) can be seen at the northern part of the domain. On June 10, this area has relaxed, and by June 30 the entire section has almost completely returned to the original state of effective pressure, around 2 MPa across the mesh. Fig. 6 depicts the channel system that is established during and after these events, showing that an area of distributed, heavy flow around 4029 and 4030 km N quickly coalesces to a narrow and efficient channel in response to higher water pressures.

So long as high fluxes continue, melt opening exceeds creep closure, keeping efficient channels open during the majority of the melt season. The drainage system is able to quickly shuttle large fluxes through, allowing it to return to a low-pressure state and draining the surrounding bed. Although velocities are not simulated here, it is inferred that sliding velocities would decrease due to a return to higher effective pressures in the summer. Beaud and others (2022)'s velocity dataset at Shishper Glacier from 2013-2019 shows that the glacier does indeed slow down significantly during summer months. In addition, increases in surface displacement further up the trunk of Shishper were observed by Bhambri and others (2020) during the early melt season (May to June) between 2013-2016, suggesting that there could be decreased effective pressures at the northern part of the domain during this time. This agrees with our model results: near the terminus, the system remains perennially channelized, while the upper part sees an inefficient, distributed system during the early melt season that evolves to become more efficient over the summer.

As the system closes and the capacity of the drainage system falls, it regains its sensitivity to temporary increases in melt, as is seen in the early and late summer spikes in hydraulic head (Fig. 5) (Hart and others, 2022). This contraction happens as basal flux falls, allowing melt opening to fall and creep closure to dominate. The spikes are smaller than the ones at the beginning of the melt season because the system has not had much time to close yet, so it is more efficient than at the beginning of spring.

Overall, these findings corroborate the established understanding that there is a transition from a distributed to channelized drainage system and back during the course of the year (Fig. 4) (Schoof, 2010; Werder and others, 2013; Flowers, 2015; Hubbard and Nienow, 1997). As long as high meltwater fluxes persist, melt opening exceeds creep closure, maintaining open channels throughout most of the melt season

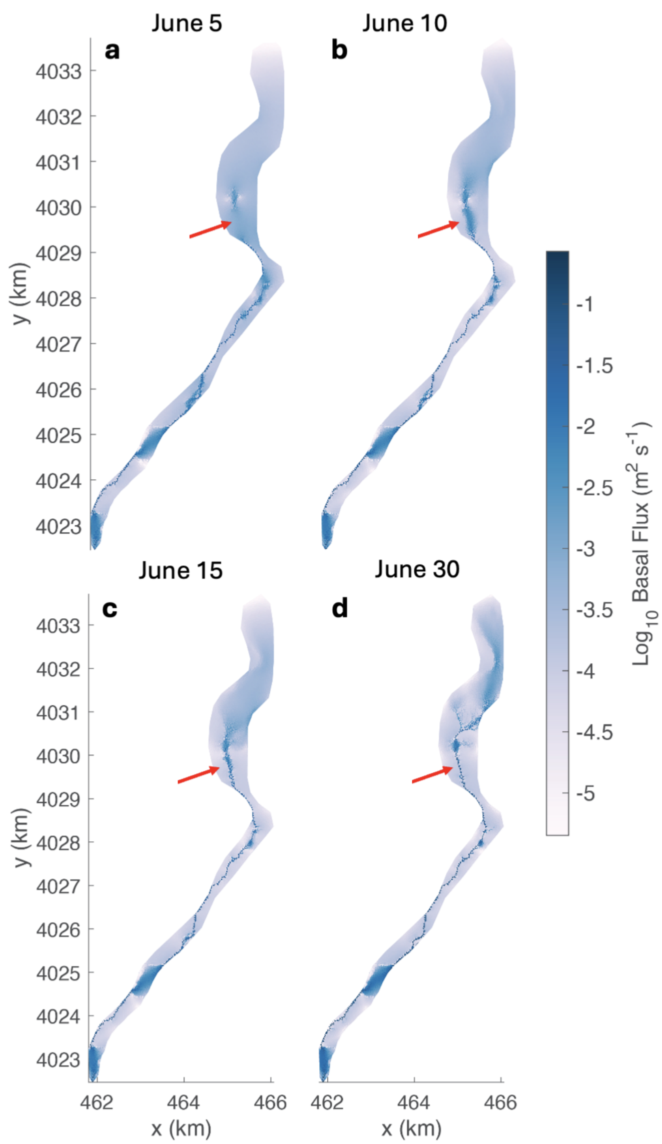

Fig. 6. Basal fluxes surrounding an early-season spike (depicted in Fig. 5) show a transition at the upper trunk from distributed, sheetlike flow to efficient, channelized flow. The red arrows highlight the formation of a channel that occurs between June 5 and June 30.

(Schoof, 2010; Werder and others, 2013; Flowers, 2015). As the system shuts down and the drainage capacity decreases toward the end of the melt season, it exhibits heightened sensitivity to melt increases, as evidenced in early and late summer hydraulic head spikes (Fig. 5) (Bartholomew and others, 2012).

SHISHPER SURGE PHASES BETWEEN 2017 AND 2019

Hydrological Insights into Surge Dynamics

Comparing the modeled effective pressures with observed surge phases implies that incipient surge motion in November 2017 and subsequent slow acceleration through the winter 2017-2018 do not show up as a clear hydrological signal in our simulations, suggesting that there could be a process or mechanism not accounted for by our model (Kamb, 1987; Björnsson, 1998). However, significant hydraulic head spikes do correspond with rapid acceleration in June 2018, suggesting that elevated water pressures could play a role in escalating already-occurring ice motion (Kamb, 1987; Björnsson, 1998).

Fig. 7 overlays effective pressure simulated by SHAKTI on top of satellite-derived velocity observations from Beaud and others (2022). Observations show a pre-surge acceleration begins in November 2017, but the model outputs indicate a decrease in effective pressure during this acceleration (Kamb, 1987; Björnsson, 1998). At the beginning of June 2018, Bhambri and others (2020) describe a rapid but brief acceleration, which corresponds to the peak of about 5.5 m d^{-1} described by Beaud and others (2022) at the same time, coinciding with a series of modeled spikes in hydraulic head at the beginning of the 2018 melt season. As the drainage system enters its efficient summer state, the surge then enters a very slow "semi-quiescent" period during which velocity is only slightly higher than normal summer velocities, lasting until September 2018 (Beaud and others, 2022). The glacier then accelerates again, reaching speeds of of approximately 2 m d^{-1} by November 2018 and 3.5 m d^{-1} in January 2019. Another surge peak occurs from late April to early May 2019 (Bhambri and others, 2020). A small GLOF of the ice-dammed lake, which damaged the Karakoram Highway, follows from June 22-23, 2019 (Bhambri and others, 2020; Beaud and others, 2022).

Our simulated spring and fall dips in effective pressure correspond with Beaud and others (2022)'s observations of spring and fall speedups at Shishper Glacier even during quiescent (non-surging) periods. The model results show larger and longer-duration effective pressure drops in spring compared to fall, aligning with observations of larger spring speedups. These spikes in hydraulic head appear more extreme than what may be expected in real life, in which localized buildups of very high water pressure would more quickly be resolved through hydraulic jacking and/or fracturing of the overlying ice. Overall, these

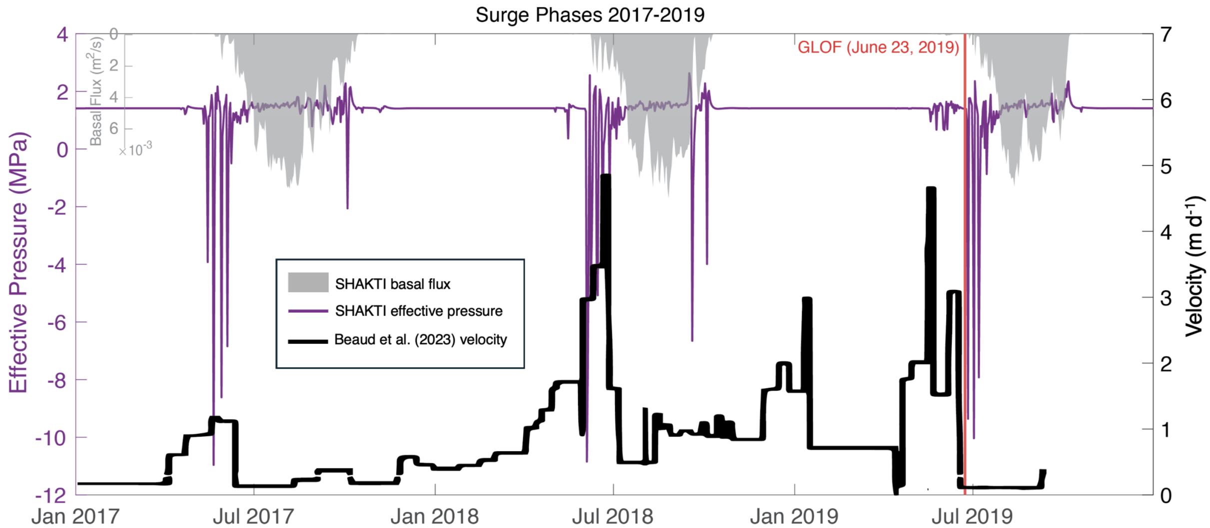

Fig. 7. Glacier surface velocities from the dataset of Beaud and others (2022) overlaid on model outputs of basal flux and effective pressure during the 2017-2019 surge. The bright red line indicates a GLOF that occurred on June 22-23, 2019.

findings support the hypotheses of observational studies suggesting that seasonal hydrology evolution is largely driving seasonal glacier motion trends in HMA (e.g., Nanni and others (2023); Sam and others (2018)).

Limitations and Future Directions

Subglacial hydrology is likely only one of several factors that may drive surge behavior. To further disentangle the drivers of surge motion, it is necessary to consider and model additional processes such as frictional feedbacks due to sliding at the ice-bed interface, basal melting due to changes in the pressure melting point, till deformation, uplift and hydrofracture, dynamic advances and retreat of the terminus, and changes in ice thickness at the reservoir and receiving zone of the glacier (e.g., Liu and others (2024); Haga and others (2020); Flowers and others (2011)). Furthermore, our model results hint that abrupt transitions from unstable, high water pressures to low (sub-flotation) pressures could play a role in slowdowns in surge motion. To quantify the role of subglacial hydrology in ice motion, a coupled model is necessary. Two-way coupling of SHAKTI with ice dynamics in ISSM has been implemented and applied recently to Helheim Glacier, Greenland (Sommers and others, 2024); implementing a similar coupled framework for this glacier could provide further insights into these complex interactions that are important for understanding the motion of surging glaciers. In addition, we have neglected the hydrological influence of upper-elevation tributary glaciers; although we do not expect large hydrological contributions from the tributaries due to their high elevation, the magnitude of hydrological flux from these tributaries may be non-trivial and ought to be considered in future work. Additional contributions from groundwater flow may also affect subglacial hydrology. Future studies should focus on integrating these processes into the model to better understand the interplay between subglacial hydrology, ice dynamics, ice-dammed lake floods, and surge behavior.

SUMMARY AND CONCLUSIONS

Our study demonstrates that subglacial hydrology plays a crucial role in modulating glacier dynamics, particularly in surge-type glaciers like Shishper. The simulations show that at least one year's melt cycle is required to bring the drainage system to a long-term equilibrium in which the subglacial drainage system returns to the same configuration every winter. This winter configuration features a primary channel in the lower trunk of the glacier which remains year-round and serves as the basis for an arborescent, channelized drainage system that grows far up the glacier as the melt season peaks.

Our simulations demonstrate SHAKTI's ability to represent the transition from an inefficient to efficient drainage pattern as melt flux rises and vice versa. These transitions are marked by large spikes in hydraulic head and corresponding dips in effective pressure, which support numerous previous observations of spring and fall speedups at Shishper and other mountain glaciers and strengthen existing hypotheses that seasonal glacier motion in High Mountain Asia is largely driven by changes in subglacial hydrology. In addition, while subglacial hydrology is widely understood to be a crucial factor behind surging, the lack of a clear hydrological trigger for incipient surge motion and for the second surge peak highlights the complexity of surge dynamics and the need for further investigation into the interactions between subglacial hydrology, ice dynamics, and other potential triggering mechanisms (Sevestre and Benn, 2015; Benn and others, 2019).

This is the first time the SHAKTI model has been applied to a realistic mountain glacier. While our simulations here involve several simplifying assumptions to focus on the evolution of subglacial hydrology in isolation from velocity coupling, the model reproduces transitions between distributed and channelized drainage that could explain the timing of spring and fall speedups in the region. This provides a solid framework for future work to expand application of the model. These future studies should focus on analyzing the complex coupling between subglacial hydrology and glacier motion (Hoffman and Price, 2014; Sommers and others, 2024). Additionally, investigating the causal link between ice-dammed lake drainage and surge termination may provide valuable insights into the role of subglacial hydrology in modulating surge behavior (Björnsson, 1998; Jiskoot and others, 2000).

DATA AVAILABILITY

ISSM (including SHAKTI) is freely available at issm.jpl.nasa.gov. Simulations were performed with ISSM version 4.24. Model output data and scripts are available in a Zenodo repository at https://doi.org/10.5281/zenodo.15644288 (Narayanan, 2025). Plots in this paper make use of ColorBrewer colormaps developed by Stephen23 (2025).

ACKNOWLEDGEMENTS

We are grateful to Yoram Terleth, an anonymous reviewer, and Editor David Rounce for their feedback which greatly improved the quality of the manuscript. We also thank Flavien Beaud for his helpful advice and velocity dataset, and Taylor Perron and Camilla Cattania for their insights. NN received support from the William Asbjornsen Albert Memorial Fellowship and the MIT Office of Graduate Education. NN and WC received support from the Heising-Simons Foundation HSF-2020-1909; ANS and CRM received support from HSF-2020-1911 and NASA grant 80NSSC24K1634.

Competing interests: The authors declare none.

REFERENCES

Anderson RS, Walder JS, Anderson SP, Trabant DC and Fountain AG (2005) The dynamic response of Kennicott Glacier, Alaska, USA, to the Hidden Creek Lake outburst flood. *Annals of Glaciology*, **40**, 237–242 (doi: 10.3189/172756405781813438)

Armstrong WH and Anderson RS (2020) Ice-marginal lake hydrology and the seasonal dynamical evolution of Kennicott Glacier, Alaska. *Journal of Glaciology*, **66**(259), 699–713 (doi: 10.1017/jog.2020.41)

Bartholomew I, Nienow P, Sole A, Mair D, Cowton T and King MA (2012) Short-term variability in Greenland Ice Sheet motion forced by time-varying meltwater drainage: Implications for the relationship between subglacial drainage system behavior and ice velocity. *Journal of Geophysical Research: Earth Surface*, **117**(F3) (doi: 10.1029/2011JF002220), _eprint: https://onlinelibrary.wiley.com/doi/pdf/10.1029/2011JF002220

Bazai N, Cui P, Carling P, Wang H and Hassan J (2022a) Increasing the episodic glacial lake outburst flood hazard in response to surge glaciers in the Karakoram. EGU22–752 (doi: 10.5194/egusphere-egu22-752), conference Name: EGU General Assembly Conference Abstracts ADS Bibcode: 2022EGUGA..24..752B

Bazai NA, Cui P, Liu D, Carling PA, Wang H, Zhang G, Li Y and Hassan J (2022b) Glacier surging controls glacier lake formation and outburst floods: The example of the Khurdopin Glacier, Karakoram. *Global and Planetary Change*, **208**, 103710 (doi: 10.1016/j.gloplacha.2021.103710)

Beaud F, Aati S, Delaney I, Adhikari S and Avouac JP (2021) Generalized sliding law applied to the surge dynamics of Shisper Glacier and constrained by timeseries correlation of optical satellite images. preprint, Glaciers/Remote Sensing (doi: 10.5194/tc-2021-96)

Beaud F, Aati S, Delaney I, Adhikari S and Avouac JP (2022) Surge dynamics of Shisper Glacier revealed by time-series correlation of optical satellite images and their utility to substantiate a generalized sliding law. *The Cryosphere*, **16**(8), 3123–3148 (doi: 10.5194/tc-16-3123-2022), publisher: Copernicus GmbH

Benn DI, Fowler AC, Hewitt I and Sevestre H (2019) A general theory of glacier surges. *Journal of Glaciology*, **65**(253), 701–716 (doi: 10.1017/jog.2019.62), publisher: Cambridge University Press

Bhambri R and 9 others (2020) The hazardous 2017–2019 surge and river damming by Shispare Glacier, Karakoram. *Scientific Reports*, **10**(1), 4685 (doi: 10.1038/s41598-020-61277-8), number: 1 Publisher: Nature Publishing Group

Bigelow DG, Flowers GE, Schoof CG, Mingo LDB, Young EM and Connal BG (2020) The Role of Englacial Hydrology in the Filling and Drainage of an Ice-Dammed Lake, Kaskawulsh Glacier, Yukon, Canada. *Journal of Geophysical Research: Earth Surface*, **125**(2), e2019JF005110 (doi: 10.1029/2019JF005110), _eprint: https://onlinelibrary.wiley.com/doi/pdf/10.1029/2019JF005110

Björnsson H (1998) Hydrological characteristics of the drainage system beneath a surging glacier. *Nature*, **395**(6704), 771–774 (doi: 10.1038/27384), number: 6704 Publisher: Nature Publishing Group

Bolch T, Pieczonka T and Benn DI (2011) Multi-decadal mass loss of glaciers in the Everest area (Nepal Himalaya) derived from stereo imagery. *The Cryosphere*, **5**(2), 349–358 (doi: 10.5194/tc-5-349-2011), publisher: Copernicus GmbH

Braithwaite RJ (2008) Temperature and precipitation climate at the equilibrium-line altitude of glaciers expressed by the degree-day factor for melting snow. *Journal of Glaciology*, **54**(186), 437–444 (doi: 10.3189/002214308785836968)

Copland L and 8 others (2009) Glacier velocities across the central Karakoram. *Annals of Glaciology*, **50**(52), 41–49 (doi: 10.3189/172756409789624229)

Copland L and 7 others (2011) Expanded and Recently Increased Glacier Surging in the Karakoram. *Arctic, Antarctic, and Alpine Research*, **43**(4), 503–516 (doi: 10.1657/1938-4246-43.4.503)

Eisen O, Harrison WD and Raymond CF (2001) The surges of Variegated Glacier, Alaska, U.S.A., and their connection to climate and mass balance. *Journal of Glaciology*, **47**(158), 351–358 (doi: 10.3189/172756501781832179), publisher: Cambridge University Press

Flowers G (2015) Modelling water flow under glaciers and ice sheets. *Proceedings of the Royal Society A: Mathematical, Physical and Engineering Sciences*, **471** (doi: 10.1098/rspa.2014.0907)

Flowers GE, Björnsson H, Pálsson F and Clarke GKC (2004) A coupled sheet-conduit mechanism for jökulhlaup propagation. *Geophysical Research Letters*, **31**(5) (doi: 10.1029/2003GL019088), _eprint: https://onlinelibrary.wiley.com/doi/pdf/10.1029/2003GL019088

Flowers GE, Roux N, Pimentel S and Schoof CG (2011) Present dynamics and future prognosis of a slowly surging glacier. *The Cryosphere*, **5**(1), 299–313 (doi: 10.5194/tc-5-299-2011)

German Aerospace Center (2018) TanDEM-X - Digital Elevation Model (DEM) - Global, 90m (doi: 10.15489/JU28HC7PUI09)

Gilbert A and 6 others (2020) The influence of water percolation through crevasses on the thermal regime of a Himalayan mountain glacier. *The Cryosphere*, **14**(4), 1273–1288 (doi: 10.5194/tc-14-1273-2020), publisher: Copernicus GmbH

Gudmundsson MT, Björnsson H and Pálsson F (1995) Changes in jökulhlaup sizes in Grímsvötn, Vatnajökull, Iceland, 1934-91, deduced from in-situ measurements of subglacial lake volume. *Journal of Glaciology*, **41**(138), 263–272 (doi: 10.3189/S0022143000016166), publisher: Cambridge University Press

Gulley J and Benn DI (2007) Structural control of englacial drainage systems in Himalayan debris-covered glaciers. *Journal of Glaciology*, **53**(182), 399–412 (doi: 10.3189/002214307783258378)

Haga ON, McNabb R, Nuth C, Altena B, Schellenberger T and Kääb A (2020) From high friction zone to frontal collapse: dynamics of an ongoing tidewater glacier surge, Negribreen, Svalbard. *Journal of Glaciology*, **66**(259), 742–754 (doi: 10.1017/jog.2020.43)

Harrison S and 14 others (2018) Climate change and the global pattern of moraine-dammed glacial lake outburst floods. *The Cryosphere*, **12**(4), 1195–1209 (doi: 10.5194/tc-12-1195-2018), publisher: Copernicus GmbH

Hart JK, Young DS, Baurley NR, Robson BA and Martinez K (2022) The seasonal evolution of subglacial drainage pathways beneath a soft-bedded glacier. *Communications Earth & Environment*, **3**(1), 1–13 (doi: 10.1038/s43247-022-00484-9), number: 1 Publisher: Nature Publishing Group

Hoffman M and Price S (2014) Feedbacks between coupled subglacial hydrology and glacier dynamics. *Journal of Geophysical Research: Earth Surface*, **119**(3), 414–436 (doi: 10.1002/2013JF002943), _eprint: https://onlinelibrary.wiley.com/doi/pdf/10.1002/2013JF002943

Hubbard B and Nienow P (1997) Alpine subglacial hydrology. *Quaternary Science Reviews*, **16**(9), 939–955 (doi: 10.1016/S0277-3791(97)00031-0)

Iken A and Bindschadler RA (1986) Combined measurements of Subglacial Water Pressure and Surface Velocity of Findelengletscher, Switzerland: Conclusions about Drainage System and Sliding Mechanism. *Journal of Glaciology*, **32**(110), 101–119 (doi: 10.3189/S0022143000006936), publisher: Cambridge University Press

Iken A, Röthlisberger H, Flotron A and Haeberli W (1983) The Uplift of Unteraargletscher at the Beginning of the Melt Season—A Consequence of Water Storage at the Bed? *Journal of Glaciology*, **29**(101), 28–47 (doi: 10.3189/S0022143000005128)

Jay-Allemand M, Gillet-Chaulet F, Gagliardini O and Nodet M (2011) Investigating changes in basal conditions of Variegated Glacier prior to and during its 1982–1983 surge. *The Cryosphere*, **5**(3), 659–672 (doi: 10.5194/tc-5-659-2011), publisher: Copernicus GmbH

Jiskoot H, Murray T and Boyle P (2000) Controls on the distribution of surge-type glaciers in Svalbard. *Journal of Glaciology*, **46**(154), 412–422 (doi: 10.3189/172756500781833115), publisher: Cambridge University Press

Kamb B (1987) Glacier surge mechanism based on linked cavity configuration of the basal water conduit system. *Journal of Geophysical Research*, **92**(B9), 9083 (doi: 10.1029/JB092iB09p09083)

Kingslake J and Ng F (2013) Modelling the coupling of flood discharge with glacier flow during jökulhlaups. *Annals of Glaciology*, **54**(63), 25–31 (doi: 10.3189/2013AoG63A331)

Kusch E and Davy R (2022) KrigR—a tool for downloading and statistically downscaling climate reanalysis data. *Environmental Research Letters*, **17**(2), 024005 (doi: 10.1088/1748-9326/ac48b3), publisher: IOP Publishing

Larour E, Seroussi H, Morlighem M and Rignot E (2012) Continental scale, high order, high spatial resolution, ice sheet modeling using the Ice Sheet System Model (ISSM). *Journal of Geophysical Research: Earth Surface*, **117**(F1) (doi: 10.1029/2011JF002140), _eprint: https://onlinelibrary.wiley.com/doi/pdf/10.1029/2011JF002140

Litt M and 6 others (2019) Glacier ablation and temperature indexed melt models in the Nepalese Himalaya. *Scientific Reports*, **9**(1), 5264 (doi: 10.1038/s41598-019-41657-5), number: 1 Publisher: Nature Publishing Group

Liu J, Enderlin EM, Bartholomaus TC, Terleth Y, Mikesell TD and Beaud F (2024) Propagating speedups during quiescence escalate to the 2020–2021 surge of Sít' Kusá, southeast Alaska. *Journal of Glaciology*, 1–12 (doi: 10.1017/jog.2023.99), publisher: Cambridge University Press

MacKie EJ, Schroeder DM, Zuo C, Yin Z and Caers J (2021) Stochastic modeling of subglacial topography exposes uncertainty in water routing at Jakobshavn Glacier. *Journal of Glaciology*, **67**(261), 75–83 (doi: 10.1017/jog.2020.84)

Miles ES and 6 others (2017) Pond Dynamics and Supraglacial-Englacial Connectivity on Debris-Covered Lirung Glacier, Nepal. *Frontiers in Earth Science*, **5** (doi: 10.3389/feart.2017.00069), publisher: Frontiers

Miles KE, Hubbard B, Quincey DJ, Miles ES, Irvine-Fynn TD and Rowan AV (2019) Surface and subsurface hydrology of debris-covered Khumbu Glacier, Nepal, revealed by dye tracing. *Earth and Planetary Science Letters*, **513**, 176–186 (doi: 10.1016/j.epsl.2019.02.020)

Miles KE and 6 others (2021) Continuous borehole optical televiewing reveals variable englacial debris concentrations at Khumbu Glacier, Nepal. *Communications Earth & Environment*, **2**(1), 1–9 (doi: 10.1038/s43247-020-00070-x), publisher: Nature Publishing Group

Millan R, Mouginot J, Rabatel A and Morlighem M (2022) Ice velocity and thickness of the world's glaciers. *Nature Geoscience*, **15**(2), 124–129 (doi: 10.1038/s41561-021-00885-z), number: 2 Publisher: Nature Publishing Group

Minchew B and 7 others (2016) Plastic bed beneath Hofsjökull Ice Cap, central Iceland, and the sensitivity of ice flow to surface meltwater flux. *Journal of Glaciology*, **62**(231), 147–158 (doi: 10.1017/jog.2016.26), publisher: Cambridge University Press

Minchew BM and Meyer CR (2020) Dilation of subglacial sediment governs incipient surge motion in glaciers with deformable beds. *Proceedings of the Royal Society A: Mathematical, Physical and Engineering Sciences*, **476**(2238), 20200033 (doi: 10.1098/rspa.2020.0033), publisher: Royal Society

Muhammad S and 8 others (2021) A holistic view of Shisper Glacier surge and outburst floods: from physical processes to downstream impacts. *Geomatics, Natural Hazards and Risk*, **12**(1), 2755–2775 (doi: 10.1080/19475705.2021.1975833), publisher: Taylor & Francis _eprint: https://doi.org/10.1080/19475705.2021.1975833

Murray T and 6 others (2000) Glacier surge propagation by thermal evolution at the bed. *Journal of Geophysical Research: Solid Earth*, **105**(B6), 13491–13507 (doi: 10.1029/2000JB900066), _eprint: https://onlinelibrary.wiley.com/doi/pdf/10.1029/2000JB900066

Muñoz-Sabater J and 16 others (2021) ERA5-Land: a state-of-the-art global reanalysis dataset for land applications. *Earth System Science Data*, **13**(9), 4349–4383 (doi: 10.5194/essd-13-4349-2021), publisher: Copernicus GmbH

Nanni U, Scherler D, Ayoub F, Millan R, Herman F and Avouac JP (2023) Climatic control on seasonal variations in mountain glacier surface velocity. *The Cryosphere*, **17**(4), 1567–1583 (doi: 10.5194/tc-17-1567-2023), publisher: Copernicus GmbH

Narayanan N (2025) Simulating Seasonal Evolution of Subglacial Hydrology at a Surging Glacier in the Karakoram (doi: 10.5281/zenodo.15644288)

Nienow PW and 6 others (2005) Hydrological controls on diurnal ice flow variability in valley glaciers. *Journal of Geophysical Research: Earth Surface*, **110**(F4) (doi: 10.1029/2003JF000112), _eprint: https://onlinelibrary.wiley.com/doi/pdf/10.1029/2003JF000112

Nye JF (1976) Water Flow in Glaciers: Jökulhlaups, Tunnels and Veins. *Journal of Glaciology*, **17**(76), 181–207 (doi: 10.3189/S002214300001354X), publisher: Cambridge University Press

Pritchard HD, King EC, Goodger DJ, McCarthy M, Mayer C and Kayastha R (2020) Towards Bedmap Himalayas: development of an airborne ice-sounding radar for glacier thickness surveys in High-Mountain Asia. *Annals of Glaciology*, **61**(81), 35–45 (doi: 10.1017/aog.2020.29)

RGI Consortium (2017) Randolph glacier inventory - a dataset of global glacier outlines, version 6 (doi: 10.7265/4M1F-GD79)

Rounce DR, Hock R and Shean DE (2020) Glacier Mass Change in High Mountain Asia Through 2100 Using the Open-Source Python Glacier Evolution Model (PyGEM). *Frontiers in Earth Science*, **7**

Round V, Leinss S, Huss M, Haemmig C and Hajnsek I (2017) Surge dynamics and lake outbursts of Kyagar Glacier, Karakoram. *The Cryosphere*, **11**(2), 723–739 (doi: 10.5194/tc-11-723-2017), publisher: Copernicus GmbH

Röthlisberger H (1972) Water Pressure in Intra- and Subglacial Channels. *Journal of Glaciology*, **11**(62), 177–203 (doi: 10.3189/S0022143000022188), publisher: Cambridge University Press

Sam L, Bhardwaj A, Kumar R, Buchroithner MF and Martín-Torres FJ (2018) Heterogeneity in topographic control on velocities of Western Himalayan glaciers. *Scientific Reports*, **8**(1), 12843 (doi: 10.1038/s41598-018-31310-y)

Schoof C (2010) Ice-sheet acceleration driven by melt supply variability. *Nature*, **468**(7325), 803–806 (doi: 10.1038/nature09618), number: 7325 Publisher: Nature Publishing Group

Scott CA, Zhang F, Mukherji A, Immerzeel W, Mustafa D and Bharati L (2019) Water in the Hindu Kush Himalaya. In P Wester, A Mishra, A Mukherji and AB Shrestha (eds.), *The Hindu Kush Himalaya Assessment: Mountains, Climate Change, Sustainability and People*, 257–299, Springer International Publishing, Cham, ISBN 978-3-319-92288-1 (doi: 10.1007/978-3-319-92288-1_8)

Setchell H (2020) ECMWF Reanalysis v5

Sevestre H and Benn DI (2015) Climatic and geometric controls on the global distribution of surge-type glaciers: implications for a unifying model of surging. *Journal of Glaciology*, **61**(228), 646–662 (doi: 10.3189/2015JoG14J136), publisher: Cambridge University Press

Shean DE, Bhushan S, Montesano P, Rounce DR, Arendt A and Osmanoglu B (2020) A Systematic, Regional Assessment of High Mountain Asia Glacier Mass Balance. *Frontiers in Earth Science*, **7** (doi: 10.3389/feart.2019.00363), publisher: Frontiers

Shengbiao H and Jiyang W (2000) Heat flow, deep temperature and thermal structure across the orogenic belts in Southeast China. *Journal of Geodynamics*, **30**(4), 461–473 (doi: https://doi.org/10.1016/S0264-3707(00)00010-7)

Shepherd A, Hubbard A, Nienow P, King M, McMillan M and Joughin I (2009) Greenland ice sheet motion coupled with daily melting in late summer. *Geophysical Research Letters*, **36**(1) (doi: 10.1029/2008GL035758), _eprint: https://onlinelibrary.wiley.com/doi/pdf/10.1029/2008GL035758

Shrestha F and 9 others (2023) A comprehensive and version-controlled database of glacial lake outburst floods in High Mountain Asia. *Earth System Science Data*, **15**(9), 3941–3961 (doi: 10.5194/essd-15-3941-2023), publisher: Copernicus GmbH

Sommers A, Rajaram H and Morlighem M (2018) SHAKTI: Subglacial Hydrology and Kinetic, Transient Interactions v1.0. *Geoscientific Model Development*, **11**(7), 2955–2974 (doi: 10.5194/gmd-11-2955-2018), publisher: Copernicus GmbH

Sommers A and 6 others (2023) Subglacial hydrology modeling predicts high winter water pressure and spatially variable transmissivity at Helheim Glacier, Greenland. *Journal of Glaciology*, 1–13 (doi: 10.1017/jog.2023.39)

Sommers AN and 7 others (2024) Velocity of Greenland's Helheim Glacier Controlled Both by Terminus Effects and Subglacial Hydrology With Distinct Realms of Influence. *Geophysical Research Letters*, **51**(15), e2024GL109168 (doi: 10.1029/2024GL109168), _eprint: https://onlinelibrary.wiley.com/doi/pdf/10.1029/2024GL109168

Steiner JF, Kraaijenbrink PDA, Jiduc SG and Immerzeel WW (2018) Brief communication: The Khurdopin glacier surge revisited – extreme flow velocities and formation of a dammed lake in 2017. *The Cryosphere*, **12**(1), 95–101 (doi: 10.5194/tc-12-95-2018), publisher: Copernicus GmbH

Stephen23 (2025) ColorBrewer: Attractive and Distinctive Colormaps

Tober BS, Christoffersen MS, Holt JW, Truffer M and Larsen CF (2024) Thickness of Ruth Glacier, Alaska, and depth of its Great Gorge from ice-penetrating radar and mass conservation. *Journal of Glaciology*, **70**, e51 (doi: 10.1017/jog.2024.53)

Werder MA, Hewitt IJ, Schoof CG and Flowers GE (2013) Modeling channelized and distributed subglacial drainage in two dimensions: A 2-D SUBGLACIAL DRAINAGE SYSTEM MODEL. *Journal of Geophysical Research: Earth Surface*, **118**(4), 2140–2158 (doi: 10.1002/jgrf.20146)

Table 1. Constants and parameter values used in this study

Symbol	Value	Units	Description
A	9.3×10^{-25}	$\mathrm{Pa}^{-3}\ \mathrm{s}^{-1}$	Flow law parameter
G	0.07	$\mathrm{W\ m}^{-2}$	Geothermal heat flux
g	9.81	$\mathrm{m\ s}^{-2}$	Gravitational acceleration
H	Varying	m	Ice thickness
L	3.34×10^5	$\mathrm{J\ kg}^{-1}$	Latent heat of fusion of water
n	3	Dimensionless	Flow law exponent
z_b	Varying	m	Bed elevation with respect to sea level
ν	1.787×10^{-6}	$\mathrm{m}^2\ \mathrm{s}^{-1}$	Kinematic viscosity of water
ω	0.001	Dimensionless	Parameter controlling nonlinear laminar/turbulent transition
ρ_i	917	$\mathrm{kg\ m}^{-3}$	Bulk density of ice
ρ_w	1000	$\mathrm{kg\ m}^{-3}$	Bulk density of water

Zhang G and 9 others (2023a) Underestimated mass loss from lake-terminating glaciers in the greater Himalaya. *Nature Geoscience*, **16**(4), 333–338 (doi: 10.1038/s41561-023-01150-1), publisher: Nature Publishing Group

Zhang G and 12 others (2024) Characteristics and changes of glacial lakes and outburst floods. *Nature Reviews Earth & Environment*, 1–16 (doi: 10.1038/s43017-024-00554-w), publisher: Nature Publishing Group

Zhang T, Wang W, An B and Wei L (2023b) Enhanced glacial lake activity threatens numerous communities and infrastructure in the Third Pole. *Nature Communications*, **14**(1), 8250 (doi: 10.1038/s41467-023-44123-z), number: 1 Publisher: Nature Publishing Group

Zheng G and 11 others (2021) Increasing risk of glacial lake outburst floods from future Third Pole deglaciation. *Nature Climate Change*, **11**(5), 411–417 (doi: 10.1038/s41558-021-01028-3), publisher: Nature Publishing Group

Zwally J, Abdalati W, Herring T, Larsen K, Saba J and Steffen K (2002) Surface Melt-Induced Acceleration of Greenland Ice-Sheet Flow. *Science*, **297**(5579) (doi: 10.1126/science.1072708)

APPENDIX A: CONSTANTS AND PARAMETER VALUES

See Table 1.

APPENDIX B: MESH RESOLUTION TESTS

We conducted a simple test of the finite element mesh resolution to ensure that the development of basal channels was not dependent on an arbitrary choice of mesh element size. We ran winter equilibrations with triangular mesh sizes of 10m, 20m, 40m, 50m, 100m, 200m, and 250m. Each was run with 6-hour timesteps for 300 days and were initialized with the same initial conditions. In Fig. 8 we show gap heights at the end of each of these winter equilibrations.

Areas of high gap height show the location of channels and subglacial lakes. The location of these channels is largely invariant with mesh resolution, suggesting that channel locations exhibit a higher dependence on topography than on mesh resolution.

APPENDIX C: SENSITIVITY TO CREEP PARAMETER A

Since the temperature at the base of Shishper is unknown, we conduct a brief sensitivity test to assess how results may change given different basal ice rheologies. In most of the simulations featured in this study, we use a value for Glen's flow law parameter A corresponding to a temperature of -5ºC (see Appendix A). Here we re-run 2017 with identical forcings but using an A value corresponding to temperate ice (0ºC). Fig. 9 shows spatially averaged means corresponding to -5ºC ice and 0ºC ice and the difference between the two.

Fig. 9 demonstrates that the timing of transitions between efficient and inefficient drainage remains the same regardless of ice softness. The amplitude of basal flux and hydraulic head remain largely the same as well; however, the amplitude of effective pressure has slightly more significant differences between the two simulations. Notably, warmer ice corresponds with less extreme spikes in effective pressure; the largest differences between the simulations occurs during the early melt season spikes.

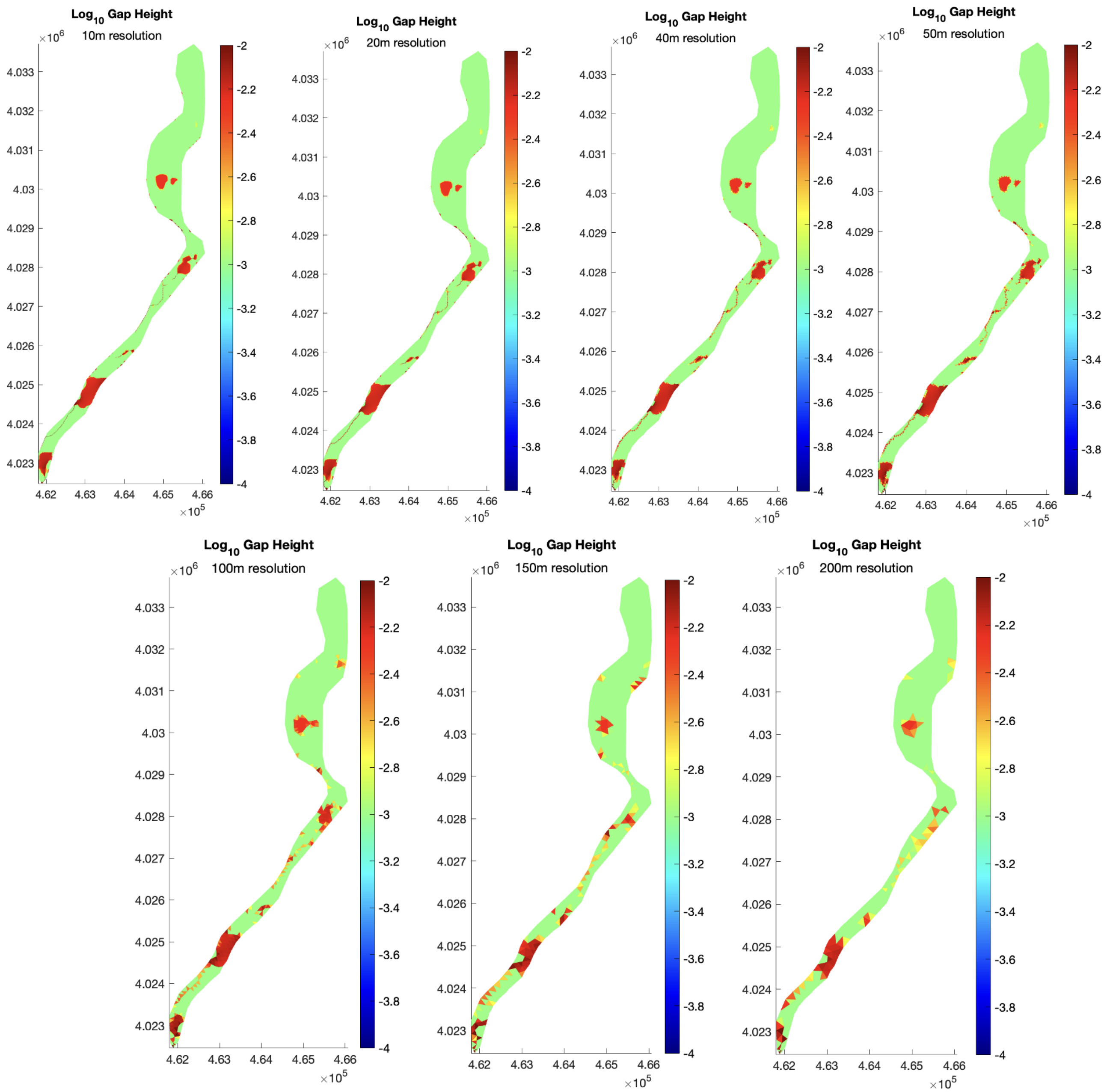

Fig. 8. Gap height (m) across the domain, shown for mesh resolutions of 10 m, 20 m, 40 m, 50 m, 100 m, 150 m, and 200 m.

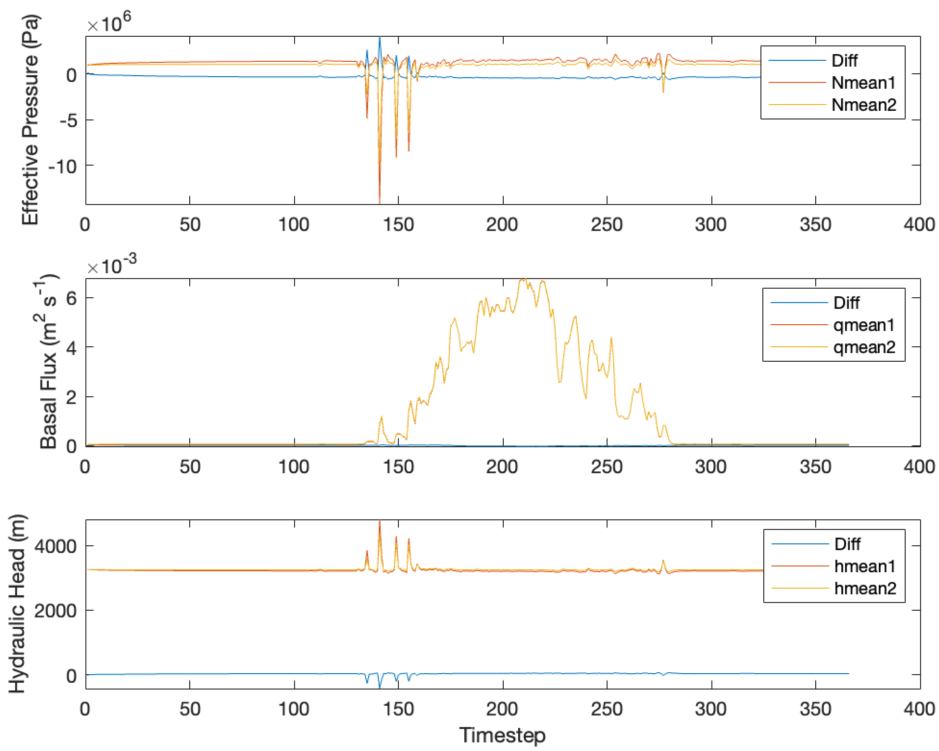

Fig. 9. Mean values for (a) effective pressure, (b) basal flux, and (c) hydraulic head. The first simulation (Nmean1, qmean1, and hmean1) was modeled with A corresponding to -5ºC while the second simulation (Nmean2, qmean2, and hmean2) used A corresponding to temperate ice (0ºC). 'Diff' refers to the difference between the two simulations.